

Signature of Pseudo Nambu-Goldstone Higgs boson in its Decay

Qing-Hong Cao,^{1,2,3,*} Ling-Xiao Xu,^{1,†} Bin Yan,^{4,‡} and Shou-hua Zhu^{1,2,3,§}

¹*Department of Physics and State Key Laboratory of Nuclear Physics and Technology, Peking University, Beijing 100871, China*

²*Collaborative Innovation Center of Quantum Matter, Beijing, 100871, China*

³*Center for High Energy Physics, Peking University, Beijing 100871, China*

⁴*Department of Physics and Astronomy, Michigan State University, East Lansing, MI 48824, USA*

If the Higgs boson is a pseudo Nambu-Goldstone boson (PNGB), the $hZ\gamma$ contact interaction induced by the $\mathcal{O}(p^4)$ invariants of the non-linear sigma model is free from its nonlinearity effects. The process $h \rightarrow Z\gamma$ can be used to eliminate the universal effects of heavy particles, which can fake the nonlinearity effects of the PNGB Higgs boson in the process $h \rightarrow V^*V$ ($V = W^\pm, Z$). We demonstrate that the ratio of the signal strength of $h \rightarrow Z\gamma$ and $h \rightarrow V^*V$ is good to distinguish the signature of the PNGB Higgs boson from Higgs coupling deviations.

Introduction. Deciphering the nature of the Higgs boson is one of the major tasks of particle physics, and one can ask whether there is dynamics behind electroweak symmetry breaking (EWSB). Given no hint of new heavy particles at the Large Hadron Collider (LHC), the best strategy is to use effective theories to parametrize the ignorance of UV physics. When the Higgs boson arises from a weakly-coupled UV theory, the Standard Model (SM) Effective Field Theory (EFT) can be used. On the other hand, the Higgs boson might emerge as a pseudo Nambu-Goldstone boson (PNGB) from some strong dynamics at the TeV scale [1–8]; see Refs. [9–11] for recent reviews. The traditional CCWZ formalism [12, 13] is often used to construct the non-linear sigma model (NL σ M) of the PNGB Higgs boson with the symmetry breaking pattern \mathcal{G}/\mathcal{H} . Alternatively, one can use the so-called shift symmetry [14, 15] to construct NL σ M even without knowing the UV group \mathcal{G} . The nature of the PNGB Higgs boson is encoded in the NL σ M, and one can characterize its signature explicitly with a parameter ξ , which is defined as the ratio of the electroweak scale v and the decay constant of the PNGB Higgs boson f . For that the parameter ξ is named as the *nonlinearity* of the PNGB Higgs boson.

It's crucial to tell whether the Higgs boson is a PNGB from Higgs precision measurements. In particular, the Higgs couplings to electroweak gauge bosons are of the most importance as they are directly related to the EWSB. Unfortunately, one cannot learn any useful information of the parameter ξ from the hVV ($V = W^\pm, Z$) couplings alone. For example, two effects could modify the hVV couplings and fake each other:

1. the nonlinearity of the PNGB Higgs boson ξ ;
2. the shift-symmetry-breaking effects induced by heavy particles, e.g. a singlet scalar interacting with the Higgs boson [16–18].

To probe the nonlinearity of the PNGB Higgs boson, we propose an observable R defined as the ratio of the signal

strengths of the $h \rightarrow Z\gamma$ and $h \rightarrow V^*V$ decay channels,

$$R \equiv \frac{\mu(h \rightarrow Z\gamma)}{\mu(h \rightarrow V^*V)}. \quad (1)$$

We demonstrate that the ratio R is sensitive only to nonlinearity of the PNGB Higgs boson in strongly-coupled models but not to the faking effects originating from unknown heavy particles. Another advantage is that R is independent of the single Higgs boson cross section and the Higgs boson width.

Higgs Couplings to Electroweak Gauge Bosons. With only the information of the group \mathcal{H} in the IR, the NL σ M of the PNGB Higgs boson can be constructed with the shift symmetry covariants $\tilde{D}_\mu H$ and \mathcal{E}_μ [14, 15]. $\tilde{D}_\mu H$ is the so-called Goldstone covariant derivative and \mathcal{E}_μ is the associated gauge fields of the shift symmetry. The constructed NL σ M is universal, up to the normalization of the PNGB decay constant f , as the PNGB Higgs boson can be embedded in different UV group \mathcal{G} . In this work, we focus on the case that \mathcal{H} contains the custodial $SO(4)$ symmetry and the PNGB Higgs boson arises from a custodial 4-plet. Below the scale of heavy resonances of the strong dynamics, the NL σ M can be expanded as

$$\mathcal{L}_{\text{NL}\sigma\text{M}} = \mathcal{O}(p^2) + \mathcal{O}(p^4) + \dots \quad (2)$$

From the operators at the order of $\mathcal{O}(p^2)$ and $\mathcal{O}(p^4)$ of the NL σ M, one can obtain the Higgs couplings to electroweak gauge bosons which respect the shift symmetry of the PNGB Higgs boson.

At the order of $\mathcal{O}(p^2)$, there is only one invariant $(\tilde{D}_\mu H)^\dagger \tilde{D}^\mu H$, which gives rise to both the normalized kinetic term of the physical Higgs boson and the mass term of the electroweak gauge bosons, i.e.

$$(\tilde{D}_\mu H)^\dagger \tilde{D}^\mu H = \frac{1}{2} \partial_\mu h \partial^\mu h + (2f^2) \frac{g^2}{4} \sin^2 \frac{\langle h \rangle + h}{\sqrt{2}f} \left(W_\mu^+ W^{-\mu} + \frac{Z^\mu Z_\mu}{2 \cos^2 \theta_W} \right), \quad (3)$$

where θ_W is the weak mixing angle and g is the gauge coupling of $SU(2)_L$ group. Matching the W^\pm and Z

masses yields the electroweak VEV as

$$v = \sqrt{2}f \sin \frac{\langle h \rangle}{\sqrt{2}f} = 246 \text{ GeV}. \quad (4)$$

Note that the VEV of the physical Higgs boson, $\langle h \rangle$, is not exactly equal to 246 GeV. We define the nonlinearity parameter ξ as

$$\xi \equiv \frac{v^2}{2f^2} = \sin^2 \frac{\langle h \rangle}{\sqrt{2}f}. \quad (5)$$

The hVV coupling is

$$\mathcal{L}_{hVV} = \frac{M_V^2}{v} \sqrt{1 - \xi} h V_\mu V^\mu, \quad (6)$$

where M_V is the mass of electroweak gauge boson V .

Although sensitive to ξ , the hVV coupling alone cannot provide enough information to pin down the Higgs boson nature; the hVV coupling could be modified by heavy particles which violate the shift symmetry [16–18]. We use SM-EFT to describe the new physics (NP) effects which violate the shift symmetry in Higgs boson physics. Only one leading operator needs to be considered at dimension-six level [19],

$$O_H = \frac{1}{2v^2} \partial_\mu (H^\dagger H) \partial^\mu (H^\dagger H). \quad (7)$$

The effect of O_H is universal in all the single Higgs boson processes as it simply rescales the amplitude as $h \rightarrow h/\sqrt{1 + c_H}$ due to the renormalization of the Higgs boson field. For cancelling the universal O_H effect, we further consider the $hZ\gamma$ coupling.

Within the NL σ M, the leading contribution to the $hZ\gamma$ effective coupling arises from the order of $\mathcal{O}(p^4)$. All the relevant $\mathcal{O}(p^4)$ operators can be derived in the CCWZ formalism with the coset $SO(5)/SO(4)$ [20, 21]. Alternatively, one can derive the $\mathcal{O}(p^4)$ operators based on the shift symmetry [22, 23]. The resultant operators are valid in any other cosets as long as there is an unbroken $SO(4)$ symmetry in the IR with a Higgs boson 4-plet. The $hZ\gamma$ effective coupling arises from two operators, $\tilde{O}_{HB} = ig'(\tilde{D}^\mu H)^\dagger(\tilde{D}^\nu H)B_{\mu\nu}$ and $\tilde{O}_{HW} = ig(\tilde{D}^\mu H)^\dagger\sigma^i(\tilde{D}^\nu H)W_{\mu\nu}^i$, which are shown as follows,

$$\begin{aligned} & ig'(\tilde{D}^\mu H)^\dagger(\tilde{D}^\nu H)B_{\mu\nu} \\ &= -\frac{gg'}{4\cos\theta_W}(\sqrt{2}f)\sin\frac{h+\langle h \rangle}{\sqrt{2}f}(\partial^\mu hZ^\nu - \partial^\nu hZ^\mu)B_{\mu\nu} \\ &\quad + \dots, \end{aligned} \quad (8)$$

$$\begin{aligned} & ig(\tilde{D}^\mu H)^\dagger\sigma^i(\tilde{D}^\nu H)W_{\mu\nu}^i \\ &= \frac{g^2}{4\cos\theta_W}(\sqrt{2}f)\sin\frac{h+\langle h \rangle}{\sqrt{2}f}(\partial^\mu hZ^\nu - \partial^\nu hZ^\mu) \\ &\quad \times (\partial_\mu W_\nu^3 - \partial_\nu W_\mu^3) + \dots, \end{aligned} \quad (9)$$

where $B_{\mu\nu}$ and $W_{\mu\nu}^3$ are the field strength tensors of external electroweak gauge bosons and g' is the gauge

coupling of the $U(1)_Y$ group. The $hZ\gamma$ coupling is

$$\begin{aligned} \mathcal{L}_{hZ\gamma} &= (\tilde{c}_{HW}\tilde{O}_{HW} + \tilde{c}_{HB}\tilde{O}_{HB})/M_W^2 \\ &= -\Delta\kappa_{Z\gamma}\tan\theta_W\frac{1}{v}(\partial^\mu hZ^\nu - \partial^\nu hZ^\mu)A_{\mu\nu}, \end{aligned} \quad (10)$$

with $\Delta\kappa_{Z\gamma} = \tilde{c}_{HB} - \tilde{c}_{HW}$. The $hZ\gamma$ coupling induced by the $\mathcal{O}(p^4)$ invariants of the NL σ M does not depend on ξ , i.e. it is not sensitive to the nonlinearity of the PNCB Higgs boson at all.

Both operators \tilde{O}_{HW} and \tilde{O}_{HB} modify the hVV and $hZ\gamma$ couplings. However, we only consider their effects in the $hZ\gamma$ coupling due to the reasons as follows. The ratio R of interest to us is

$$R = \frac{\mu(h \rightarrow Z\gamma)}{\mu(h \rightarrow V^*V)} \propto \frac{g_{hZ\gamma}}{g_{h\gamma}^{\text{SM}}} \cdot \frac{g_{hVV}^{\text{SM}}}{g_{hVV}}, \quad (11)$$

where $g_{hZ\gamma}^{\text{SM}}$ ($g_{hZ\gamma}$) and g_{hVV}^{SM} (g_{hVV}) denotes the couplings of $hZ\gamma$ and hVV in the SM (NP), respectively. The hVV coupling is generated at tree level while the $hZ\gamma$ coupling at one loop level in the SM. To match the same precision of the SM couplings, the sub-leading correction to hVV coupling from \tilde{O}_{HW} and \tilde{O}_{HB} are neglected due to the loop suppression [19]. Similarly all the operators are considered in the $h \rightarrow Z\gamma$ decay.

There is another loop-induced and shift-symmetry breaking operator $O_\gamma \sim H^\dagger H B_{\mu\nu} B^{\mu\nu}$ contributing to the processes of $h \rightarrow Z\gamma$ and $h \rightarrow \gamma\gamma$. Its contribution is tightly constrained by the precision measurements of $h\gamma\gamma$ coupling, however. We thus neglect the contribution of O_γ in $h \rightarrow Z\gamma$ in this work.

The Ratio R . Next we show the observable R , the ratio of the signal strengths of $h \rightarrow Z\gamma$ and $h \rightarrow V^*V$, is sensitive only to the nonlinearity of the PNCB Higgs boson but not to the faking effects of O_H .

The leading corrections to the signal strength of the process $h \rightarrow V^*V$ from both the nonlinearity of the PNCB Higgs boson and the O_H operator are

$$\begin{aligned} \mu(h \rightarrow V^*V) &= \frac{\sigma_h \times \text{BR}(h \rightarrow V^*V)}{\sigma_h^{\text{SM}} \times \text{BR}(h \rightarrow V^*V)_{\text{SM}}} \\ &= \frac{\sigma_h}{\sigma_h^{\text{SM}}} \cdot \frac{\Gamma_{\text{total}}^{\text{SM}}}{\Gamma_{\text{total}}} \cdot F_{\text{PNCB}} \cdot F_{O_H}, \end{aligned} \quad (12)$$

where

$$F_{\text{PNCB}} = 1 - \xi, \quad F_{O_H} = \frac{1}{1 + c_H}. \quad (13)$$

Here, σ_h (σ_h^{SM}) and Γ_{total} ($\Gamma_{\text{total}}^{\text{SM}}$) denotes the single Higgs boson production cross section and the Higgs boson total width in NP models (the SM), respectively. The substitution of $\xi \rightarrow -\xi$ describes a PNCB Higgs boson from various non-compact groups [15, 24]. It is clear that one cannot distinguish the contribution from F_{PNCB} and F_{O_H} in the $h \rightarrow VV^*$ decays.

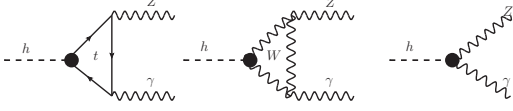


FIG. 1. Illustrative Feynman diagrams of $h \rightarrow Z\gamma$. The black dots denote the effective couplings including both the SM and NP effects.

TABLE I. The NP effect in the hVV and $hZ\gamma$ couplings when the Higgs boson is a PNBG or a SM-like scalar ($\xi \rightarrow 0$) from weakly-coupled UV theories. The symbol \checkmark and \times means that the NP effect could and cannot contribute, respectively.

hVV	PNBG	SM-like	$hZ\gamma$	PNBG	SM-like
ξ -effect	\checkmark	\times	ξ -effect	\times	\times
O_H	\checkmark	\checkmark	O_H	\checkmark	\checkmark

For the process of $h \rightarrow Z\gamma$ there are contributions from the top-quark loop, the W -boson loops and the $hZ\gamma$ effective coupling; see Fig. 1. NP effects that modify the hWW and $ht\bar{t}$ effective couplings are also included. The partial width of the $h \rightarrow Z\gamma$ decay is

$$\Gamma(h \rightarrow Z\gamma) = F_{O_H} \frac{M_h^3}{8\pi v^2} \left(1 - \frac{M_Z^2}{M_h^2}\right)^3 \times \left|F_{Z\gamma}^t + F_{Z\gamma}^W \sqrt{F_{\text{PNBG}}} + \Delta\kappa_{Z\gamma} \tan\theta_W\right|^2, \quad (14)$$

where M_h and M_Z denotes the masses of the Higgs boson and the Z boson, respectively. $F_{Z\gamma}^W$ and $F_{Z\gamma}^t$ represents the loop effects of the W -boson and top-quark in the SM. Note that the W -boson loop dominates over the top-quark loop, e.g. $F_{Z\gamma}^W = 0.0087$ and $F_{Z\gamma}^t = -0.00097$. The signal strength of $h \rightarrow Z\gamma$ is

$$\begin{aligned} \mu(h \rightarrow Z\gamma) &= \frac{\sigma_h \times \text{BR}(h \rightarrow Z\gamma)}{\sigma_h^{\text{SM}} \times \text{BR}(h \rightarrow Z\gamma)_{\text{SM}}} \\ &= \frac{\sigma_h}{\sigma_h^{\text{SM}}} \cdot \frac{\Gamma_{\text{total}}^{\text{SM}}}{\Gamma_{\text{total}}} \cdot F_{O_H} \\ &\times \frac{|F_{Z\gamma}^t + F_{Z\gamma}^W \sqrt{F_{\text{PNBG}}} + \Delta\kappa_{Z\gamma} \tan\theta_W|^2}{|F_{Z\gamma}^t + F_{Z\gamma}^W|^2}, \end{aligned} \quad (15)$$

where the O_H effect (F_{O_H}) is factorized out.

The ratio R follows from Eqs. (12) and (15) as

$$R = \frac{|F_{Z\gamma}^t + F_{Z\gamma}^W \sqrt{F_{\text{PNBG}}} + \Delta\kappa_{Z\gamma} \tan\theta_W|^2}{|F_{Z\gamma}^t + F_{Z\gamma}^W|^2 F_{\text{PNBG}}}. \quad (16)$$

The dependence of σ_h and Γ_{total} cancels out in the ratio R , and, more important, the F_{O_H} term also cancels out. Table I shows the impact of both the Higgs nonlinearity and the O_H operator on the hVV and $hZ\gamma$ effective couplings, depending on whether the Higgs boson is a PNBG from strong dynamics at $\sim \text{TeV}$ scale or a SM-like scalar from weakly-coupled UV theories ($\xi \rightarrow 0$).

The $hZ\gamma$ effective coupling is crucial to eliminate the universal effect of O_H so as to extract out the nonlinearity (ξ) of the PNBG Higgs boson.

One thus can determine F_{PNBG} when both the $\Delta\kappa_{Z\gamma}$ and R are known precisely from data; for example, F_{PNBG} follows directly from Eq. 16 as

$$F_{\text{PNBG}} = \left(\frac{F_{Z\gamma}^t + \Delta\kappa_{Z\gamma} \tan\theta_W}{\sqrt{R}|F_{Z\gamma}^t + F_{Z\gamma}^W| - F_{Z\gamma}^W} \right)^2 \simeq \left(\frac{\Delta\kappa_{Z\gamma} \tan\theta_W}{(\sqrt{R} - 1)F_{Z\gamma}^W} \right)^2 \quad (17)$$

when $\sqrt{F_{\text{PNBG}}} > 0.11 - 0.6 \times \left(\frac{\Delta\kappa_{Z\gamma}}{0.01}\right)$, or as

$$F_{\text{PNBG}} = \left(\frac{F_{Z\gamma}^t + \Delta\kappa_{Z\gamma} \tan\theta_W}{\sqrt{R}|F_{Z\gamma}^t + F_{Z\gamma}^W| + F_{Z\gamma}^W} \right)^2 \simeq \left(\frac{\Delta\kappa_{Z\gamma} \tan\theta_W}{(\sqrt{R} + 1)F_{Z\gamma}^W} \right)^2 \quad (18)$$

when $\sqrt{F_{\text{PNBG}}} < 0.11 - 0.6 \times \left(\frac{\Delta\kappa_{Z\gamma}}{0.01}\right)$, where the approximations can be understood by $F_{Z\gamma}^W \gg |F_{Z\gamma}^t|$. For a sizable ξ one might be able to tell the PNBG Higgs boson apart from a SM-like scalar (i.e. $F_{\text{PNBG}} = 1$). If the Higgs boson is a PNBG, F_{PNBG} could be smaller than one or larger than one, depending on a specific UV group from which the PNBG Higgs boson emerges; for example, $F_{\text{PNBG}} < 1$ for a compact UV group ($\xi > 0$) and $F_{\text{PNBG}} > 1$ for a non-compact UV group ($\xi < 0$) [24]. It is fascinating that the ratio R distinguishes the compactness of the broken UV-group \mathcal{G} 's.

Figure 2(a) displays the contour of F_{PNBG} in the plane of R and $\Delta\kappa_{Z\gamma}$ for $F_{\text{PNBG}} = 0.7$ (black), 1.0 (red) and 1.3 (blue). Figure 2(b) shows the dependence of F_{PNBG} on R for various $\Delta\kappa_{Z\gamma}$'s. We note that the discrimination power of F_{PNBG} increases with R and is strong for a negative $\Delta\kappa_{Z\gamma}$ but quite weak for positive $\Delta\kappa_{Z\gamma}$'s. For example, the blue dashed curve ($\Delta\kappa_{Z\gamma} = 0.01$) in Fig. 2(b) is not sensitive to F_{PNBG} .

Sensitivity at the LHC and CEPC. Now consider the potential of measuring F_{PNBG} at the High luminosity Large Hadron Collider (HL-LHC), a proton-proton collider to operate at $E_{\text{cm}} = 14 \text{ TeV}$ with an integrated luminosity of 3 ab^{-1} [25], and also at the Circular

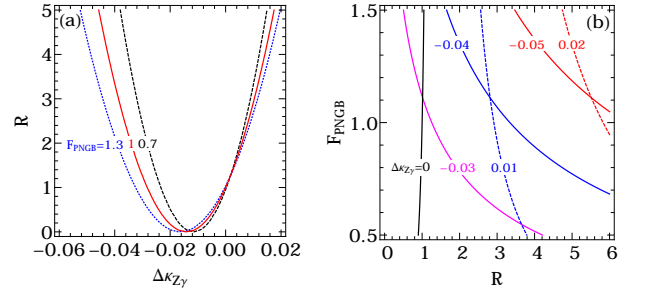


FIG. 2. The correlations among F_{PNBG} , R and $\Delta\kappa_{Z\gamma}$. Shown is the contour line of one parameters in the plane of the other twos.

electron-positron collider (CEPC), proposed to operate at $E_{\text{cm}} = 240$ GeV with an integrated luminosity of 5 ab^{-1} [26].

The coefficient $\Delta\kappa_{Z\gamma}$ can be derived from the measurement of anomalous triple gauge-boson couplings (aTGCs) [27, 28]

$$\mathcal{L}_{\text{TGC}}/g_{WWV} = ig_{1,V} \left(W_{\mu\nu}^+ W_\mu^- \nabla_\nu - W_{\mu\nu}^- W_\mu^+ \nabla_\nu \right) + i\kappa_V W_\mu^+ W_\nu^- \nabla_{\mu\nu} + \frac{i\lambda_V}{M_W^2} W_{\lambda\mu}^+ W_{\mu\nu}^- \nabla_{\nu\lambda}, \quad (19)$$

where $\nabla = \gamma/Z$, $g_{WW\gamma} = -e$ and $g_{WWZ} = -e \cot \theta_W$. The NP contributions in the $g_{1,Z}$ and $\Delta\kappa_\gamma$ are

$$\begin{aligned} \Delta g_{1,Z} &\equiv g_{1,Z} - 1 = \tilde{c}_{HW} / \cos^2 \theta_W, \\ \Delta\kappa_\gamma &\equiv \kappa_\gamma - 1 = \tilde{c}_{HW} + \tilde{c}_{HB}. \end{aligned} \quad (20)$$

It follows that

$$\Delta\kappa_{Z\gamma} = \tilde{c}_{HB} - \tilde{c}_{HW} = \Delta\kappa_\gamma - 2\Delta g_{1,Z} \cos^2 \theta_W. \quad (21)$$

$\Delta\kappa_\gamma$ and $\Delta g_{1,Z}$ are expected to be measured with precisions as follows [29]:

$$\begin{aligned} \delta\kappa_\gamma &= 0.0029 \text{ (HL-LHC)}, \quad 0.00022 \text{ (CEPC)}, \\ \delta g_{1,Z} &= 0.0011 \text{ (HL-LHC)}, \quad 0.00016 \text{ (CEPC)}. \end{aligned} \quad (22)$$

The uncertainty $\delta\kappa_{Z\gamma}$,

$$\delta\kappa_{Z\gamma} = \sqrt{\delta\kappa_\gamma^2 + 4 \cos^4 \theta_W \delta g_{1,Z}^2},$$

is given by

$$\delta\kappa_{Z\gamma} = 0.0033 \text{ (HL-LHC)}, \quad 0.00034 \text{ (CEPC)}. \quad (23)$$

The uncertainty of the ratio R is

$$\frac{\delta R}{R_0} = \sqrt{\left(\frac{\delta\mu_{h \rightarrow Z\gamma}}{\mu_{h \rightarrow Z\gamma}^0} \right)^2 + \left(\frac{\delta\mu_{h \rightarrow VV^*}}{\mu_{h \rightarrow VV^*}^0} \right)^2}, \quad (24)$$

where R_0 , $\mu_{h \rightarrow Z\gamma}^0$ and $\mu_{h \rightarrow VV^*}^0$ denotes the central values of R , $\mu(h \rightarrow Z\gamma)$ and $\mu(h \rightarrow VV^*)$, respectively. The signal strengths $\mu(h \rightarrow Z\gamma)$ and $\mu(h \rightarrow VV^*)$ are expected to be measured at the HL-LHC [30, 31] and the CEPC [32] with errors as follows:

$$\begin{aligned} \delta\mu_{h \rightarrow Z\gamma} &= 0.3 \text{ (HL-LHC)}, \quad 0.25 \text{ (CEPC)}, \\ \delta\mu_{h \rightarrow VV^*} &= 0.1 \text{ (HL-LHC)}, \quad 0.01 \text{ (CEPC)}. \end{aligned} \quad (25)$$

For simplicity we assume $\mu_{h \rightarrow VV^*}^0 = 1$ (i.e. no deviation in the hVV couplings), yielding

$$\delta R = \sqrt{(\delta\mu_{h \rightarrow Z\gamma})^2 + R_0^2 (\delta\mu_{h \rightarrow VV^*})^2}. \quad (26)$$

Defining F_{PNGB}^0 and $\Delta\kappa_{Z\gamma}^0$ as the central values of F_{PNGB} and $\Delta\kappa_{Z\gamma}$, respectively, the error of F_{PNGB} is

$$\frac{\delta\sqrt{F_{\text{PNGB}}}}{\sqrt{F_{\text{PNGB}}^0}} = \sqrt{\left(\frac{\delta\kappa_{Z\gamma}}{\Delta\kappa_{Z\gamma}^0} \right)^2 + \left(\frac{\delta\sqrt{R}}{\sqrt{R_0} \mp 1} \right)^2}$$

$$\simeq 0.32 \times \sqrt{\left(\frac{\delta\kappa_{Z\gamma}}{0.003} \right)^2 \left(\frac{0.01}{\Delta\kappa_{Z\gamma}^0} \right)^2 + \left(\frac{\delta R}{0.3} \right)^2 \frac{1}{4R_0(\sqrt{R_0} \mp 1)^2}}, \quad (27)$$

where we normalize the errors with the HL-LHC projections and the sign “ \mp ” refers to Eqs. 17 and 18. A large R_0 would suppress the effects δR and we expect to reach a better measurement of F_{PNGB} . The typical error of F_{PNGB} is about 30% at the HL-LHC, while it reduces to $\sim 3\%$ at the CEPC.

Figure 3 displays the sensitivity to F_{PNGB} from the R and $\Delta\kappa_{Z\gamma}$ measurements at the HL-LHC (a, b) and the CEPC (c, d). The latest global fit results of Higgs boson couplings show that the ξ value is highly constrained [33, 34]. As both the Higgs nonlinearity and heavy new resonances can contribute to Higgs coupling deviations, these two effects might accidentally cancel each other out. We choose three benchmark values of F_{PNGB} 's for illustration; $F_{\text{PNGB}} = 0.7$ (black-dashed curve) and $F_{\text{PNGB}} = 1.3$ (blue-dashed) describes a PNGB Higgs boson from a compact and non-compact UV group, respectively, while $F_{\text{PNGB}} = 1.0$ (red-solid) denotes a SM-like Higgs boson. The shade band along each $F_{\text{PNGB}} = 1.0$ curve represents the 68% C.L. uncertainty of the F_{PNGB} measurement, which is derived from Eq. 27. The black cross denotes a benchmark point of $(\Delta\kappa_{Z\gamma}, R)$ and the corresponding errors given by Eqs. 23 and 26. The green and yellow shaded regions are not allowed

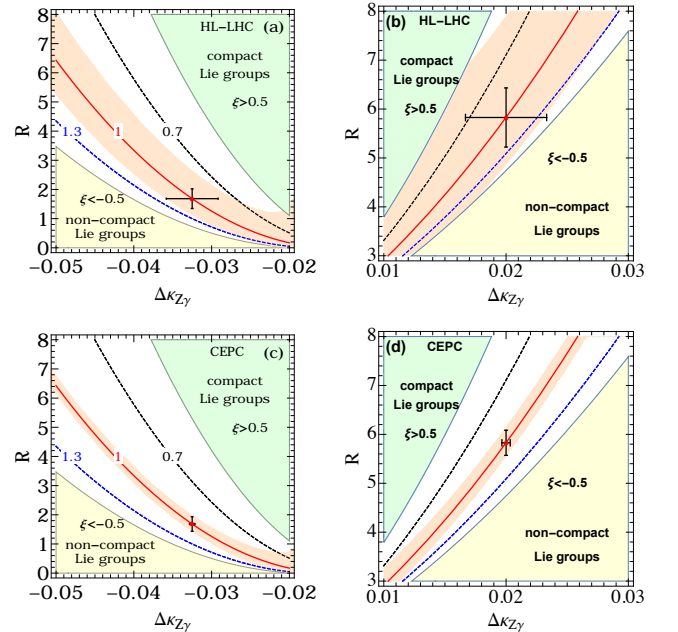


FIG. 3. The sensitivity to F_{PNGB} at the HL-LHC (a, b) and the CEPC (c, d). The black (blue) dashed curve denotes the contour of $F_{\text{PNGB}} = 0.7$ (1.3), respectively. The red curve represents the $F_{\text{PNGB}} = 1$ contour with a 68% C.L. error band. The green and yellow regions are excluded for $|\xi| \geq 0.5$.

as $|\xi|$ is too large ($|\xi| \geq 0.5$). Equipped with precision measurements of aTGCs and Higgs-boson couplings, one could determine $F_{\text{PNGB}} = 1.0 \pm (0.15 \sim 0.25)$ at the HL-LHC in the regions of $\Delta\kappa_{Z\gamma} \lesssim -0.03$ and $R \gtrsim 1$; see Fig. 3(a). However, it is not possible to do so for a positive $\Delta\kappa_{Z\gamma}$; see Fig. 3(b). In comparison with the HL-LHC, the uncertainty of aTGCs measurements at the CEPC is reduced by a factor of 10; see Eqs. (27). As a result, the sensitivity to F_{PNGB} at the CEPC is improved greatly; for example, given a sizable R , one can determine $F_{\text{PNGB}} = 1.0 \pm (0.03 \sim 0.1)$ in the negative $\Delta\kappa_{Z\gamma}$ region and $F_{\text{PNGB}} = 1.0 \pm (0.05 \sim 0.25)$ in the positive $\Delta\kappa_{Z\gamma}$ region. For a sizeable ξ , we could distinguish the Higgs boson nature since the accuracy of F_{PNGB} is much improved at the CEPC.

Conclusions. In this letter, we propose the signature of the PNGB Higgs boson can be distinguished in the ratio of $\mu(h \rightarrow VV^*)$ and $\mu(h \rightarrow Z\gamma)$ with the help of precision measurements of anomalous triple-gauge-boson couplings. The contribution of O_H in the SM-EFT, which fakes the nonlinearity effect in $h \rightarrow VV^*$, is canceled out. Our result is valid in any coset \mathcal{G}/\mathcal{H} , as long as the unbroken group \mathcal{H} in the IR contains the custodial $SO(4)$, of which the Higgs boson arises from a custodial 4-plet. Depending on the magnitude of Higgs boson nonlinearity parameter ξ , at least 1σ confidence level of experimental sensitivity can be reached in general with the prospected accuracy of $h \rightarrow Z\gamma$, $h \rightarrow V^*V$, aTGCs at HL-LHC and CEPC. Especially for the negative region of $\Delta\kappa_{Z\gamma}$, the sensitivity is good at the CEPC because aTGCs can be measured very accurately.

Acknowledgements. We thank Da Liu, Yandong Liu, Ian Low, Zhewei Yin, C.-P. Yuan, Chen Zhang, Hao Zhang for helpful conversations and Jiang-Hao Yu, Jue Zhang for comments on the manuscript. This work is supported in part by the National Science Foundation of China under Grants No. 11635001, 11275009, 11675002, 11725520 and 11875072. BY is supported by the U.S. National Science Foundation under Grant No. PHY-1719914.

* qinghongcao@pku.edu.cn

† lingxiaoxu@pku.edu.cn

‡ yanbin1@msu.edu

§ shzhu@pku.edu.cn

- [1] D. B. Kaplan and H. Georgi, Phys. Lett. **136B**, 183 (1984).
- [2] D. B. Kaplan, H. Georgi, and S. Dimopoulos, Phys. Lett. **136B**, 187 (1984).
- [3] M. J. Dugan, H. Georgi, and D. B. Kaplan, Nucl. Phys. **B254**, 299 (1985).
- [4] N. Arkani-Hamed, A. G. Cohen, and H. Georgi, Phys. Lett. **B513**, 232 (2001), hep-ph/0105239.
- [5] N. Arkani-Hamed, A. G. Cohen, E. Katz, and A. E. Nelson, JHEP **07**, 034 (2002), hep-ph/0206021.
- [6] R. Contino, Y. Nomura, and A. Pomarol, Nucl. Phys. **B671**, 148 (2003), hep-ph/0306259.
- [7] K. Agashe, R. Contino, and A. Pomarol, Nucl. Phys. **B719**, 165 (2005), hep-ph/0412089.
- [8] Z. Chacko, H.-S. Goh, and R. Harnik, Phys. Rev. Lett. **96**, 231802 (2006), hep-ph/0506256.
- [9] R. Contino (2011), 1005.4269.
- [10] B. Bellazzini, C. Csaki, and J. Serra, Eur. Phys. J. **C74**, 2766 (2014), 1401.2457.
- [11] G. Panico and A. Wulzer, Lect. Notes Phys. **913**, pp.1 (2016), 1506.01961.
- [12] S. R. Coleman, J. Wess, and B. Zumino, Phys. Rev. **177**, 2239 (1969).
- [13] C. G. Callan, Jr., S. R. Coleman, J. Wess, and B. Zumino, Phys. Rev. **177**, 2247 (1969).
- [14] I. Low, Phys. Rev. **D91**, 105017 (2015), 1412.2145.
- [15] I. Low, Phys. Rev. **D91**, 116005 (2015), 1412.2146.
- [16] I. Low, R. Rattazzi, and A. Vichi, JHEP **04**, 126 (2010), 0907.5413.
- [17] S. Dawson and C. W. Murphy, Phys. Rev. **D96**, 015041 (2017), 1704.07851.
- [18] T. Corbett, A. Joglekar, H.-L. Li, and J.-H. Yu, JHEP **05**, 061 (2018), 1705.02551.
- [19] G. F. Giudice, C. Grojean, A. Pomarol, and R. Rattazzi, JHEP **06**, 045 (2007), hep-ph/0703164.
- [20] R. Contino, D. Marzocca, D. Pappadopulo, and R. Rattazzi, JHEP **10**, 081 (2011), 1109.1570.
- [21] A. Azatov, R. Contino, A. Di Iura, and J. Galloway, Phys. Rev. **D88**, 075019 (2013), 1308.2676.
- [22] D. Liu, I. Low, and Z. Yin (2018), 1805.00489.
- [23] D. Liu, I. Low, and Z. Yin (2018), 1809.09126.
- [24] R. Alonso, E. E. Jenkins, and A. V. Manohar, Phys. Lett. **B756**, 358 (2016), 1602.00706.
- [25] G. Apollinari, I. Bjar Alonso, O. Brning, M. Lamont, and L. Rossi, *High-Luminosity Large Hadron Collider (HL-LHC): Preliminary Design Report*, CERN Yellow Reports: Monographs (CERN, Geneva, 2015), URL <https://cds.cern.ch/record/2116337>.
- [26] M. Ahmad et al. (CEPC-SPPC Study Group), *CEPC-SPPC Preliminary Conceptual Design Report. 1. Physics and Detector* (2015), URL http://cepc.ihep.ac.cn/preCDR/main_preCDR.pdf.
- [27] A. De Rujula, M. B. Gavela, P. Hernandez, and E. Masso, Nucl. Phys. **B384**, 3 (1992).
- [28] K. Hagiwara, S. Ishihara, R. Szalapski, and D. Zeppenfeld, Phys. Rev. **D48**, 2182 (1993).
- [29] L. Bian, J. Shu, and Y. Zhang, JHEP **09**, 206 (2015), 1507.02238.
- [30] Tech. Rep. ATL-PHYS-PUB-2014-006, CERN, Geneva (2014), URL <https://cds.cern.ch/record/1703276>.
- [31] Tech. Rep. CMS-NOTE-13-002, CERN-CMS-NOTE-2013-002, CERN, Geneva (2013), snowmass 2013 - Energy Frontier Contributed papers, URL <http://cds.cern.ch/record/1565454>.
- [32] G. Durieux, C. Grojean, J. Gu, and K. Wang, JHEP **09**, 014 (2017), 1704.02333.
- [33] G. Aad et al. (ATLAS, CMS), JHEP **08**, 045 (2016), 1606.02266.
- [34] Tech. Rep. ATLAS-CONF-2018-031, CERN, Geneva (2018), URL <http://cds.cern.ch/record/2629412>.